Trophoblast uptake of DBP regulates intracellular actin and promotes matrix invasion

Ankana Ganguly[1], Jennifer A. Tamblyn[1,2,3], Alexandra Shattock[1], Annsha Joseph[1], Dean P. Larner[1], Carl Jenkinson[1], Janesh Gupta[1,2], Stephane R. Gross[4], Martin Hewison[1,3]

[1]Institute of Metabolism and Systems Research, the University of Birmingham, Birmingham B15 2TT, UK
[2]Birmingham Women's & Children's Foundation Hospital Trust, Mindelsohn Way. Edgbaston. Birmingham. B15 2TGUK
[3]CEDAM, Birmingham Health Partners, the University of Birmingham, Birmingham B15 2TT, UK
[4]School of Life and Health Sciences, Aston University, Birmingham B4 7ET, UK

* Corresponding author:
Martin Hewison PhD
Institute of Metabolism & Systems Research
Level 2, IBR, Rm 225
The University of Birmingham
Birmingham, B15 2TT
UK
email: m.hewison@bham.ac.uk
Tel: +44 (0)121 414 6908
Fax: +44 (0) 121 415 8712

Running title: DBP, intracellular actin and matrix invasion

Key words: vitamin D, vitamin D binding protein, pregnancy, placenta, trophoblast, actin

Word count: 5,000

Abstract

Early pregnancy is characterised by elevated circulating levels of vitamin D binding protein (DBP). The impact of this on maternal and fetal health is unclear but DBP is present in the placenta, and DBP gene variants have been linked to malplacentation disorders such as preeclampsia. A functional role for DBP in the placenta was investigated using trophoblastic JEG3, BeWo and HTR8 cells. All three cells lines showed intracellular DBP, with increased expression and nuclear localisation of DBP in cells treated with the active form of vitamin D, 1,25-dihydroxyvitamin D (1,25D). When cultured in serum from mice lacking DBP (DBP-/-), JEG3 cells showed no intracellular DBP indicating uptake of exogenous DBP. Inhibition of the membrane receptor for DBP, megalin, also suppressed intracellular DBP. Elimination of intracellular DBP with DBP-/- serum or megalin inhibitor suppressed matrix invasion by trophoblast cells, and was associated with increased nuclear accumulation of G-actin. Conversely, treatment with 1,25D enhanced matrix invasion. This was independent of the nuclear vitamin D receptor but was associated with enhanced ERK phosphorylation, and inhibition of ERK kinase suppressed trophoblast matrix invasion. When cultured with serum from pregnant women, trophoblast matrix invasion correlated with DBP concentration, and DBP was lower in first trimester serum from women who later developed preeclampsia. These data show that trophoblast matrix invasion involves uptake of serum DBP and associated intracellular actin binding and homeostasis. DBP is a potential marker of placentation disorders such as preeclampsia and may also provide a therapeutic option for improved placenta and pregnancy health.

Word count: 250

Introduction

Vitamin D binding protein (DBP) is a serum globulin associated with systemic transport of vitamin D metabolites (Chun 2012). Glomerular filtration of DBP and its primary cargo, the main circulating form of vitamin D, 25-hydroxyvitamin D (25D), play a pivotal role in vitamin D endocrinology. Recovery of the DBP-25D complex from glomerular filtrate by proximal convoluted tubular cells of the kidney occurs via endocytic uptake of DBP utilising the megalin receptor. This recovery of 25D from glomerular filtrates faciltates renal conversion of 25D to active 1,25-dihydroxyvitamin D (1,25D) (Nykjaer, et al. 1999), via the vitamin D-activating enzyme 1α-hydroxylase (CYP27B1), which is also expressed by proximal tubule cells (Zehnder, et al. 1999). Although only 5% of DBP molecules have vitamin D metabolites bound at any given time, megalin-mediated uptake of DBP in proximal tubules also functions to maintain circulating levels of 25D. Mice with knockout of the DBP (*Gc*) (Safadi, et al. 1999) or megalin (*Lrp2*) genes (Nykjaer et al. 1999) have extremely low serum levels of 25D, and single nucleotide polymorphisms (SNPs) of the human DBP gene (*GC*) are major contributors to the genetic component of serum 25D status (Wang, et al. 2010).

Megalin is present at several extra-renal sites (Lundgren, et al. 1997), including the placenta (Burke, et al. 2013), where its expression is coincident with DBP (Ma, et al. 2012). Both maternal decidua and fetal trophoblast also express CYP27B1 and the intracellular vitamin D receptor (VDR) for 1,25D (Zehnder, et al. 2001). Thus, the placenta, like the kidney, has a significant capacity for vitamin D metabolism that may be supported by megalin-mediated DBP transport. Circulating levels of 1,25D (Kumar, et al. 1979) and DBP (Jorgensen, et al. 2004) are increased during early pregnancy but the precise function of DBP in the placenta is unclear and may involve known vitamin D-independent functions of DBP. These include a potential role as a macrophage-activation factor (Benis and Schneider 1996), and in fatty acid transport (Calvo and Ena 1989). DBP also binds the monomeric, globular, form of actin (G-actin) with high affinity, allowing DBP to compete with other established actin-regulating factors such as gelsolin which incorporates G-

actin into filamentous actin (F-actin)(Otterbein, et al. 2002). In this way, DBP can also function as a systemic actin-scavenger, with a potential role in protecting against tissue damage due to systemic F-actin accumulation (Luebbering, et al. 2020), although the DBP-actin complex may also fulfil a pro-inflammatory role as a neutrophil chemotactic factor (Kew 2019).

Variations in serum vitamin D metabolites (Bodnar, et al. 2007; Wei, et al. 2013) and SNPs for *GC* (Baca, et al. 2018; Naidoo, et al. 2019) have been linked to adverse events in pregnancy such as the malplacentation disorder preeclampsia but the mechanisms underpinning these associations remain unclear. In particular, although DBP and vitamin D metabolites are abundant in the placenta, their role in placental development has yet to be defined. In the current study we show that trophoblast cells internalize extracellular DBP and that this process is essential for trophoblast matrix invasion. Decreased cellular uptake of DBP was associated with increased nuclear accumulation of G-actin and decreased capacity for trophoblast matrix invasion. The concentration of DBP in serum from pregnant women correlated with capacity for trophoblast matrix invasion in *ex vivo* assays, and DBP levels in first trimester pregnancy serum samples were significantly lower in women who developed preeclampsia later in pregnancy. These data indicate that serum DBP is a crucial circulating factor in early pregnancy. Trophoblast uptake of maternal DBP may be pivotal to early placental development, with dysregulation of this process leading to associated disorders of placentation such as preeclampsia.

Materials and methods

Cell culture and reagents

Choriocarcinoma trophoblastic cells lines JEG3 and BeWo (European Collection of Authenticated Cell Cultures), non-neoplastic first trimester extravillous like trophoblasts cells HTR8 (a kind gift from Dr S. Gross, Aston University) were routinely cultured at 37°C and 5% CO_2 in MEM (Sigma Aldrich), DMEM/F12 Ham (1:1) with HEPES (Thermo Fisher Scientific), and RPMI-1640 Medium

110 W/L-Glutamine (Thermo Fisher) respectively, each supplemented with 10% fetal bovine serum
111 (FBS) (Thermo Fisher Scientific). Thyroid papillary carcinoma (TPC) cell line (a kind gift from
112 Prof. CJ McCabe, University of Birmingham) was cultured in RPMI-1640 Medium W/L-Glutamine
113 (Thermo Fisher) supplemented with 10% FBS. Cells were cultured on growth factor reduced
114 Matrigel pre-coated transwell plates (Corning® BioCoat™ Matrigel®, 8.0 micron). All cells were
115 treated for 2-72 hours (h) with vehicle (0.1% ethanol), 1,25D (1-100 nM) (Enzo Lifesciences), DBP
116 (East Coast Bio) (3 μM), the megalin inhibitor receptor associated protein (RAP), (1 μM) Enzo
117 Life Sciences) or the ERK-inhibitor U0126 (1 μM) (Cell Signalling).

118118

119 Cell proliferation

120 All cells were seeded at a concentration of $5x10^3$ cells/ well in a 24-well plate, and proliferation
121 assessed by quantification of nuclear incorporation of 5-bromo-2-deoxyuridine (BrdU) using a
122 BrdU assay kit as per manufacturer's instructions (Cell Signalling Technology).

123123

124 Matrix invasion

125 Cell invasion of matrix was evaluated using growth-factor-reduced Matrigel-coated transwells. All
126 cells were treated with pre-warmed culture medium containing 2% FBS for 24 h prior to passage.
127 Cell were then trypsinised, re-suspended in 2% FBS culture medium and $5x10^4$ cells per well
128 seeded onto transwell inserts in the upper chamber of each well. Complete media (with 10% FBS)
129 was added to the lower chamber of each transwell. Immediately after seeding cells were treated
130 according to specific experiments for a further 48 h. The lower surface of the transwell inserts was
131 then washed with PBS then 95% ethanol and stained with Haematoxylin (Sigma), followed by
132 washing with Scott's water, and further staining with Eosin-Y (VWR chemicals). After further
133 washes with 70% ethanol and 99% ethanol, transwell Matrigel inserts were dried at room
134 temperature, and the lower surface of each insert imaged using a microscope (Leica DM ILM
135 inverted) at x10 magnification. Under blinded conditions, 5 images per well were taken for each

136 well and the number of invaded cells were manually counted for each image. Each transwell was
137 imaged 5 times at 5 different image quadrants.
138138
139 In some experiments, quantification of invaded cells in the Matrigel transwell assays was carried
140 out using Crystal violet (Sigma) to stain the invading cells, and acetic acid to solubilise the 1%
141 Crystal violet stain. Cell seeding and incubation were carried out as described above. Invaded
142 cells on the transwell were washed twice with PBS, then stained with 1% crystal violet for 10min,
143 and then washed again with PBS. Following this, transwell inserts were left to dry at room
144 temperature. Images of each insert were taken for counting (5 quadrants per transwell as
145 explained above). Transwell inserts were then immersed in 400 µl 30% acetic acid (in 24 well
146 plate) and shaken for 10 min at room temperature. Following this, 100 µl of the blue stained acetic
147 acid solution was pipetted into triplicate wells in a 96 well plate and absorbance measured at 590
148 nm and 405 nm (OD value) using an ELISA plate reader (SpectraMax ABS, Molecular devices,
149 San Jose). Each experiment was repeated multiple times as indicated and values reported as
150 percentage (%). The total number of cells invading through transwell was calculated by converting
151 absorbance values to cell numbers using a standard curve with known cell numbers. Percentage
152 invasion was obtained by dividing the number of cells invaded by the number of cells seeded.
153153

154 Quantitative RT-PCR

155 Total RNA was extracted from cell cultures using Trizol reagent (Sigma Aldrich, Lot no.
156 BCBV4616) as per manufacturer's instructions. For each sample, 200-400 ng RNA was then
157 reverse transcribed using a Reverse Transcription Kit (Thermo Fisher Scientific, 4368814)
158 according to the manufacturer's instruction, and cDNAs amplified for the following genes: vitamin
159 D receptor (*VDR*) (Thermo Fisher, Hs00172113_m1); 24-hydroxylase (*CYP24A1*) (Thermo
160 Fisher, Hs00167999_m1); vitamin D binding protein (*DBP*/*Gc*) (Thermo Fisher,
161 Hs00167096_m1); Matrix metalloproteinase 2 (*MMP2*) (Thermo Fisher, Hs01548727_m1);

162 Tissue inhibitor of metalloproteinase 1 (*TIMP1*) (Thermo Fisher, Hs01092512_g1); megalin/*LRP2*
163 (Thermo Fisher Hs00189742_m1); *Beta-actin* (Hs01060665_g1), *GAPDH* (Hs02758991_g1) and
164 18S rRNA (Hs99999901_s1) were used as housekeeping internal standards. cDNA amplification
165 was carried out using GoTaq qPCR MasterMix (ThermoFisher, 4318157) in a thermocycler
166 (GeneAmp PCR System 2700, ThermoFisher Scientific) with amplification at 50 °C for 2 min and
167 95 °C for 10 min followed by 40 cycles of 95 °C for 15 s and 60 °C for 1 min. Differences in mRNA
168 expression were assessed statistically using raw δCt values VDR mRNA Where δCt= Ct target
169 gene – Ct housekeeping gene. Expression of mRNA was expressed visually as 1/ δCt.

170170

171 Western Blot Analysis

172 Whole cell protein lysates were extracted using radioimmunoprecipitation assay (RIPA) buffer
173 (with Tris-EDTA) with protease and phosphatase inhibitor. Cytoplasmic and nuclear proteins were
174 fractionated using NE-PER nuclear and cytoplasmic extraction reagents (Thermo Fisher
175 Scientific), per manufacturer instructions. Proteins were separated using SDS-polyacrylamide
176 (10%) gel electrophoresis, transferred to nitrocellulose membranes, and probed with various
177 antibodies using chemiluminescence (Pierce ECL Plus, Thermo Fisher Scientific). Proteins
178 quantified by Western blotting were: VDR (Santa Cruz, D-6), DBP (Abcam), ERK1/2
179 (ThermoFisher, MA5-15134, K.913.4), pERK 1/2 (ThermoFisher,MA5-15173, S.812.9). β-actin
180 (Abcam) was used as housekeeping control protein for whole cell lysates and cytoplasmic
181 proteins (**Supplemental Table 1**). Lamin B1 (Abcam) was used as a housekeeping protein for
182 nuclear lysates, and Na-K-ATPase (Abcam) was used as a housekeeping protein for membrane
183 lysates. Secondary antibodies used were goat anti-mouse HRP (Abcam), and goat anti-rabbit
184 HRP (Abcam).

185185

186 Immunofluorescence analysis of cellular protein expression

187 Cells were cultured on coverslips or Matrigel transwell inserts using 2% FBS culture medium. The
188 resulting monolayers were washed x3 with PBS and fixed in 3% paraformaldehyde at room
189 temperature for 20 min. Cells were then incubated for 10 min in chilled 100% methanol or Triton
190 X-100 (Sigma) according to the antibody used. This was followed by a PBS wash and blocking
191 with 10% neonatal calf serum (N4637) for 30 min. Incubation with primary antibody
192 (**Supplemental Table 1**) in 1% bovine serum albumin (Merck) in PBS was then carried out for 1
193 h at room temperature, followed x3 washes with PBS. Preparations were then incubated with
194 secondary antibody or Hoechst stain for nucleus (Invitrogen) at 1:1000 dilution, mixed with 1%
195 neonatal calf serum and 1% bovine serum albumin. Secondaries used were Alexa Fluor 488 -
196 conjugated goat anti-mouse IgG (ThermoFisher) and Alexa Fluor 594 -conjugated goat anti-rabbit
197 IgG (ThermoFisher, A11037) at 1:250 dilution, for each coverslip. Following this, the conjugated
198 antibodies were mixed with 1% neonatal calf serum and 1% bovine serum albumin, and the
199 samples were incubated for 1 h in these antibodies. This was followed by washing 3 times with
200 PBS. The coverslips and the Matrigel transwell base were then mounted on Thermo Fisher
201 ProLong™ Diamond Antifade Mountant media (ThermoFisher). Slides were imaged with Confocal
202 Microscope Zeiss LSM 780, and analysed and quantified using ImageJ Fiji (NIH, USA).
203 Expression levels for target proteins were determined using ImageJ Fiji software (NIH, USA) by
204 measuring "area of fluorescence colour" subtracted from "integrated density", then multiplied by
205 "average background area", and reported as corrected total cell fluorescence (CTCF).

206206

207 siRNA knockdown of VDR

208 VDR siRNA was used to knockdown *VDR* mRNA expression in JEG3 and TPC cells. ON-
209 TARGETplus Human *VDR* (7421 siRNA (Dharmacon, L-003448-00-0010) was used for *VDR*
210 knockdown at a concentration of 100 nM. A scrambled sequence siRNA (Ambion, 4390843) (100
211 nM) was included as a negative control. Transfections were performed in transwells (24 wells)
212 coated with Matrigel. In an Eppendorf tube, 250 µl of Opti-MEM reduced serum medium (Gibco

213 ThermoFisher) and 6µl Lipofectamine RNAiMAX transfection reagent (ThermoFisher) were
214 combined and incubated for 5 min at room temperature. Following this, 2.5 µl of siRNA per well
215 was added to the solution and incubated for 20 minutes. 500µl of the above final solution was
216 then added to each well (100 nM siRNA concentration, from a stock solution of 40 µM) and cells
217 incubated for 48 h. All transfections were performed with 10,000 cells seeded on Matrigel and
218 cultured for 48 h. Transfection medium was then replaced with respective regular cell culture
219 medium prior to immunofluorescence and/or invasion assay. Each experiment was carried out in
220 triplicate and repeated multiple times.

221221

222 Analysis of serum DBP concentrations

223 Human serum samples from pregnant women were obtained from two sources. The first set of
224 samples were obtained as part of previous studies of maternal serum and placental/ decidual
225 concentrations of vitamin D metabolites and DBP in 1st, 2nd and 3rd trimester pregnancies (Ethics:
226 14/WM/1146, obtained from West Midlands - Edgbaston Research Ethics Committee) (Tamblyn,
227 et al. 2017). For these samples, serum, placental and decidual human DBP concentrations were
228 previously determined (Tamblyn et al. 2017), and serum samples were used to prepare patient
229 specific JEG3 Matrigel invasion assays. The second set of samples were obtained from University
230 of Cork, Cork, Ireland as part of a study to assess vitamin D metabolite concentrations in serum
231 and urine from pregnant women at 1st trimester of pregnancy, 50% of whom went on to develop
232 preeclampsia (Clinical Research Ethics Committee of the Cork Teaching Hospital:
233 ECM5(10)05/02/08), amendment 14/WM/1146 - RG_14-194 2 and material transfer agreement
234 15.04.2016 15-1386)(Tamblyn, et al. 2018). Using these samples, an ELISA (Enzyme-linked
235 Immune Sorbent Assay) Kit (K2314, Immundiagnostik, Bensheim was used to quantify serum
236 concentrations of DBP as previously reported (Tamblyn et al. 2017).

237237

238 Statistics

239 All experiments were carried out in replicate wells according to experiment and repeated 3 to 4
240 times with separate cultures as indicated. One-Way ANOVA and *t*-test (parametric data) was
241 performed with mean and the 95% confidence interval (GraphPad PRISM (Version 8.0, La Jolla, CA). A *p*-
242 value of <0.05 was considered statistically significant.

243243

244 Results

245 DBP and VDR are present in trophoblasts cultured on Matrigel

246 VDR and DBP were detectable in JEG3, BeWo and HTR8 trophoblasts, as well as TPC thyroid
247 carcinomas cells (**Figure 1A**). VDR expression was significantly lower in TPC cells compared to
248 trophoblastic cells (**Figure 1B**), but increased in these cells with 1,25D. Both trophoblast and TPC
249 cells showed significant induction of DBP expression with 1,25D (**Figure 1B**).

250250

251 1,25D promotes trophoblast matrix invasion

252 Although trophoblasts expressed VDR, mRNA for the VDR-target gene *CYP24A1* was
253 undetectable in JEG3, BeWo and HTR8 cells even in the presence of 1,25D (**Figure 2A**). By
254 contrast, vehicle-treated TPC cells showed low *CYP24A1* mRNA, which increased dramatically
255 with 1,25D. TPC cells also showed a significant antiproliferative response to 1,25D, whereas
256 JEG3, BeWo and HTR8 cells showed no response (**Figure 2B**). For JEG3, BeWo and HTR8 cell
257 Matrigel invasion increased significantly following treatment with 1,25D, whilst 1,25D inhibited
258 matrix invasion by TPC cells (**Figure 2C**). Pro-invasive effects of 1,25D on trophoblast cells were
259 associated with increased expression of *MMP2* and decreased expression of its inhibitor, *TIMP1*.
260 By contrast, the anti-invasion effect of 1,25D (100 nM) on TPC cells was associated with
261 decreased *MMP2* and increased *TIMP1* expression (**Figure 2D**).

262262

263 Knockdown of VDR protein (**Figure 3A** and **3B**) using siRNA had no effect on JEG3 Matrigel
264 invasion in the presence or absence of 1,25D (**Figure 3C**). In TPC cells, knockdown of VDR
265 suppressed Matrigel invasion significantly, but treatment with 1,25D did not suppress invasion in
266 VDR knockdown TPC cells. These data indicate that the stimulation of trophoblast matrix invasion
267 by 1,25D is not dependent on VDR expression.

268268

269 Intracellular expression of DBP is due to uptake of serum DBP

270 JEG3 cells cultured in medium supplemented with serum from wild type (DBP+/+) mice showed
271 low levels of expression of the gene for DBP (*GC*) and the DBP membrane receptor megalin
272 (*LRP3*) (**Figure 4A**). Expression of mRNA for *GC* and *LRP2* was enhanced significantly following
273 treatment with 1,25D. JEG3 cells cultured in medium supplemented with serum from DBP
274 knockout (DBP-/-) mice showed lower baseline expression of *GC* and *LRP2* relative to cells
275 cultured with DBP+/+ serum. Expression of LRP3 in JEG3 cells cultured with DBP-/- serum was
276 enhanced by treatment with 1,25D in a similar fashion to DBP+/+ cells (**Figure 4A**). DBP+/+
277 serum-cultured JEG3 cells also expressed protein for DBP and megalin, but DBP protein
278 expression was significantly decreased in cells cultured with DBP-/- serum (**Figure 4B** and **4C**).
279 By contrast, megalin protein levels increased in DBP-/- JEG3 cells (**Figure 4C**). These data
280 suggest that although JEG3 cells express low levels of mRNA for *GC* and *LRP2*, the presence of
281 DBP protein in these cells is dependent on uptake of exogenous DBP from serum.

282282

283 JEG3 cells cultured in medium with serum from DBP-/- mice showed significantly lower matrix
284 invasion than cells cultured with DBP+/+ serum (p=0.0007). Unlike DBP+/+ cells, cells cultured in
285 DBP-/- serum showed no enhanced invasion response when treated with 1,25D (**Figure 4D**).
286 Decreased invasion by JEG3 cells cultured in DBP-/- medium was characterised by decreased
287 expression of mRNA for matrix metalloproteinase 2 (*MMP2*) and, unlike DBP+/+ cultures, DBP-/-
288 cells showed no *MMP2* response to 1,25D (**Figure 4E**). Conversely, DBP-/- cultures of JEG3 cells

showed higher levels of mRNA for tissue inhibitor of metalloproteinase-1 (*TIMP1*) than DBP+/+ cells. Both DBP+/+ and DBP-/- cultures showed suppressed *TIMP1* in the presence of 1,25D.

JEG3 cells treated with the megalin inhibitor RAP showed decreased expression of DBP (**Figure 4F** and **4G**). Although RAP acts to inhibit endocytic internalisation of megalin-DBP, it also suppressed cellular expression of megalin (**Figure 4F** and **4G**), consistent with previously reported studies (Birn, et al. 2000). JEG3 cells incubated with the megalin-inhibitor RAP also showed significantly lower levels of Matrigel invasion relative to vehicle-treated cells (**Figure 4H**). These data indicate that inhibition of cellular uptake of DBP via megalin profoundly suppresses matrix invasion by JEG3 cells.

Effects of DBP and 1,25D on trophoblast matrix invasion involve ERK phosphorylation

Previous studies have shown that enhanced matrix invasion by trophoblasts following treatment with 1,25D involves intracellular ERK signalling (Kim, et al. 2018). JEG3, BeWo and HTR8 trophoblasts showed increased nuclear phosphorylated ERK (pERK) following treatment with 1,25D (**Figure 5A**), and cytoplasmic and nuclear pERK were blocked when the cells were incubated with the ERK inhibitor U0126 in the presence or absence of 1,25D (**Figure 5A** and **5B**). U0126 also blocked intracellular uptake of DBP into JEG3 cells but had no effect on VDR expression (**Figure 5C**). Co-treatment with 1,25D partially abrogated suppressive effects of U0126 on intracellular DBP in JEG3 cells (**Figure 5C**). Similar results were also obtained for BeWo and HTR8 cells (**Supplemental Figure 1**). In JEG3, BeWo and HTR8 cells U0126 suppressed Matrigel invasion, and this was unaffected by co-treatment with 1,25D (**Figure 5D**). In TPC cells, U0126 had no effect on matrix invasion by TPC cells with or without 1,25D.

Intracellular DBP in trophoblasts acts to regulate accumulation of nuclear G-actin

314 DBP binds vitamin D metabolites with high affinity but is also a potent scavenger of G-actin
315 (Delanghe, et al. 2015). Immunofluorescence analysis of F-actin and G-actin in JEG3 and HTR8
316 cells cultured in medium supplemented with either DBP+/+ or DBP-/- serum showed different
317 patterns of intracellular actin. In the presence of extracellular DBP (DBP+/+ serum) cells showed
318 only low levels of G-actin but this increased significantly in cells cultured without DBP (DBP-/-
319 serum) (**Figure 6A** and **6B**). Lack of DBP was also associated with decreased cellular F-actin in
320 JEG3 and HTR8 cells (**Figure 6B**). In the absence of DBP, the ratio of G-actin/F-actin increased
321 from 0.62 to 2.19 in JEG3 cells and 0.18 to 0.60 in HTR8 cells (**Figure 6C**).

322322

323 **Serum concentrations of DBP and 1,25D define matrix invasion by trophoblasts**

324 Serum concentrations of maternal 1,25D and DBP increase during pregnancy but vary
325 considerably within cohorts (Tamblyn et al. 2017). To assess the impact of these two factors on
326 trophoblast matrix invasion, serum from 14 women in the first trimester of pregnancy was used to
327 generate individual JEG3 Matrigel invasion cultures. Data in **Figure 7A** showed that serum DBP
328 concentrations correlate significantly with Matrigel invasion by JEG3 cells. There was also a trend
329 for correlation between invasion and serum levels of 1,25D (**Figure 7B**), but no correlation with
330 serum 25D (**Figure 7C**). When normalised to serum levels of 1,25D, DBP concentrations showed
331 an even stronger correlation with trophoblast invasion (**Figure 7D**), but no similar effect was
332 observed when DBP was normalised to 25D concentrations (**Figure 7E**).

333333

334 These data indicate that serum levels of both DBP and 1,25D can influence trophoblast matrix
335 invasion. To determine possible clinical implications of this observation, concentrations of DBP
336 were analysed in serum samples from a cohort of first trimester pregnancies in which 50% of
337 women went on to have normal healthy deliveries, whilst 50% went on to develop the hypertensive
338 disorder preeclampsia. Data in **Figure 7F** showed that women with healthy pregnancies had

339 significantly higher serum DBP (mean: 869.5 ng/ml, 95% CI: 812.7 – 919.1) than women who
340 developed preeclampsia (mean: 691.4 ng/ml, 95% CI: 647.2 – 735.6).
341341

342 **Discussion**

343 We have shown previously that placental levels of DBP correlate directly with maternal circulating
344 DBP across gestation (Tamblyn et al. 2017). In the current study, we show that although
345 trophoblast cells express low levels of *GC* mRNA, the presence of DBP protein in these cells is
346 due primarily to megalin-mediated endocytic uptake. Megalin and its co-receptor cubilin have
347 been shown to be expressed by trophoblastic tissues within the placenta (Akour, et al. 2013), by
348 primary cultures of trophoblasts (Longtine, et al. 2017), and by trophoblast cell lines cultured on
349 Matrigel (Akour, et al. 2015). Interestingly, preliminary analysis of trophoblastic cells cultured
350 using conventional plasticware indicates that these cells do not exhibit intracellular DBP
351 (**Supplemental Figure 2**). Thus, interaction with matrix components may be a key factor in
352 cellular acquisition of DBP, presumably via enhanced expression of megalin. Although the
353 promiscuous nature of megalin-mediated endocytosis means that it is involved in the placental
354 transport of a wide range of potential ligands (Akour et al. 2013), its role in DBP uptake by placenta
355 cells is still not clear. Here we show that inhibition of DBP uptake by either ablation of DBP in
356 serum, or inhibition of megalin suppressed Matrigel invasion by JEG3 cells, highlighting an
357 entirely new function for DBP as an intracellular regulator of cell invasion.
358358

359 Trophoblastic uptake of DBP may facilitate the cellular movement and metabolism of vitamin D
360 within the placenta. The transfer of 25D and 1,25D from mother to fetus is thought to occur by
361 passive diffusion of these lipid soluble molecules across the placenta (Ryan and Kovacs 2020).
362 However, the presence of megalin in placental tissues (Burke et al. 2013; Ma et al. 2012),
363 suggests that transport of vitamin D metabolites across the placenta may be facilitated by binding
364 of DBP and its cargo to megalin. In the current study, we have highlighted an additional potential

consequence of placental uptake of DBP. In the circulation serum DBP also functions as a potent actin-binder (Otterbein et al. 2002) protecting against tissue damage due to systemic F-actin accumulation (Gomme and Bertolini 2004). In recent studies using alpha-cells of the Islets of Langerhans we have shown that cytoplasmic DBP also participates in intracellular actin homeostasis, with concomitant effects on glucagon secretion (Viloria, et al. 2020). We therefore postulated that DBP in trophoblast cells interacts with intracellular actin in a similar fashion. The cellular actions of G- and F-actin are complex, and actin homeostasis plays a crucial role in regulating cell differentiation and function (Skruber, et al. 2018). A reduced G-/F-actin ratio has been associated with increased matrix invasion by trophoblast giant cells (Chakraborty and Ain 2018). In the current study we show that in the absence of DBP there is a 4-5-fold increase in the G-/F-actin ratio for JEG3 and HTR8 cells, and this is associated with decreased matrix invasion by these cells. Our data also suggest that the increased intracellular G-actin and decreased matrix invasion in the absence of DBP specifically reflect increased nuclear G-actin expression. Nuclear actin is known to regulate cell differentiation and function (Misu, et al. 2017), but it remains to be determined if this plays a role in trophoblast cell biology and, in particular, matrix invasion. It is also possible that DBP acts to modulate actin polymerization to F-actin, and decreased actin polymerization has been shown to impair trophoblast cell matrix invasion (Liang, et al. 2019).

DBP may play a pivotal role in coordinating the intracellular functions of both G- and F-actin in trophoblast cells, but this activity appears to be distinct from intracellular DBP in other cell types. In islets of Langerhans, the presence of DBP is due to alpha-cell-specific expression of the DBP gene (*GC*), rather than cellular uptake of circulating DBP. Using islets isolated from wild type (DBP+/+) and *GC* knockout (DBP-/-) mice we showed that loss of intracellular DBP was associated with decreased alpha-cell size and glucagon release, with indirect effects on beta-cell insulin release (Viloria et al. 2020). The ratio of G-/F-actin is known to be important for secretory function of islet cells (Kalwat and Thurmond 2013), and DBP-/- alpha-cells showed a shift from

391 monomeric G-actin expression to increased F-actin (Viloria et al. 2020). Thus in alpha-cells
392 intracellular DBP appears to function by limiting DBP for polymerization to F-actin, while in
393 trophoblasts DBP appears to limit nuclear uptake of G-actin. This dichotomy of function may
394 reflect the endogenous nature of DBP and its specific secretory function of alpha-cells but,
395 nevertheless, underlines the importance of DBP for maintenance of both systemic and
396 intracellular actin homeostasis. This is further illustrated by previously reported studies of hepatic
397 stellate cells which do not express DBP/*GC* but acquire DBP in a megalin-dependent fashion from
398 hepatocytes which express and secrete DBP (Gressner, et al. 2008). After internalization by
399 hepatic stellate cells, DBP acts to bind intracellular actin, with concomitant effects on
400 transdifferentiation of these cells into myofibroblasts (Gressner et al. 2008).

401401

402 Although DBP plays a pivotal role in defining the matrix invasion by trophoblastic cells, our data
403 also indicate a role for DBP's cargo. Active vitamin D, 1,25D, promoted trophoblast matrix
404 invasion consistent with previous studies of trophoblast cells (Chan, et al. 2015; Kim et al. 2018).
405 This effect was independent of the nuclear VDR and trophoblast cells did not exhibit classical
406 1,25D-VDR responses such as induction of *CYP24A1*, but instead promoted non-nuclear
407 signalling via induction of pERK. This mechanism is required for trophoblast responses to 1,25D,
408 but also appears to play a fundamental role in promoting trophoblast invasion in general. Inhibition
409 of pERK dramatically suppressed matrix invasion by all three trophoblast cell lines in the presence
410 or absence of 1,25D, and this was associated with complete suppression of intracellular DBP and
411 elevation of nuclear G-actin. Thus, megalin-mediated uptake of DBP by trophoblasts appears to
412 be dependent on ERK phosphorylation, with increased pERK following treatment with 1,25D
413 acting to further enhance matrix invasion. By contrast, in thyroid carcinoma TPC cells 1,25D
414 suppressed matrix invasion, and these cells also demonstrated classical nuclear responses to
415 1,25D, similar to those described for 1,25D and other tumor cells lines (Bao, et al. 2006). Thus,
416 the action of 1,25D in promoting matrix invasion by trophoblast cells is distinct from more

417 established cellular anti-proliferative/anti-invasion effects of vitamin D, and acts to amplify the
418 actions of cellular DBP uptake.
419419
420 Data in **Figure 4** and **Figure 5** suggest that DBP and its ligand 1,25D act in a coordinated fashion
421 to optimise trophoblast invasion. To test this hypothesis, we used serum from healthy 1st trimester
422 pregnancies to assess matrix invasion capacity for individual pregnant women. The observation
423 that serum DBP levels alone are sufficient to define the magnitude of JEG3 matrix invasion
424 underlined the importance of DBP as a determinant of healthy placenta development. We have
425 shown previously that placental levels of DBP are directly proportional to maternal serum
426 concentrations of DBP (Tamblyn et al. 2017). Data presented here suggest that this, in turn, plays
427 a key role in directing trophoblast function. Although maternal serum 1,25D showed only a trend
428 towards enhanced matrix invasion by JEG3 cells, adjustment of DBP concentrations to account
429 for 1,25D resulted in a stronger correlation with invasion than for DBP alone. Collectively these
430 data endorse a mechanistic model in which 1,25D acts to promote DBP uptake and enhance
431 trophoblast invasion. Nevertheless, in 1st trimester serum samples DBP concentration alone was
432 sufficient to discriminate between women who went on to healthy pregnancies and those who
433 developed preeclampsia. This is in stark contrast to measurement of vitamin D metabolites such
434 as 25D and 1,25D which showed no difference between these two populations of women
435 (Tamblyn et al. 2018). It is also important to recognise that in serum invasion experiments serum
436 25D had no impact on matrix invasion by JEG3 cells, even when used to adjust DBP levels.
437 Serum 25D levels are used almost exclusively as the marker of vitamin D 'status' for studies of
438 human health. Based on data presented in the current study, we propose that this approach is an
439 oversimplification of the biological action of vitamin D, with both DBP and active 1,25D
440 coordinating important molecular, cellular and clinical actions of vitamin D.
441441

Data presented here suggest an entirely new paradigm for vitamin D and placental function in which the serum vitamin D carrier DBP plays a pivotal role in trophoblast matrix invasion (**Figure 8**). The fact that trophoblasts acquire exogenous DBP from using megalin-mediated endocytosis provides a mechanism by which circulating maternal levels of DBP can influence fetal trophoblast function. Serum DBP concentrations are increased in pregnant versus non-pregnant women but the function of this is unclear. We propose that lower serum levels of DBP during pregnancy may impair matrix invasion by fetal trophoblasts. Consistent with this we show that circulating 1st trimester levels of DBP are lower in women who go on to develop the malplacentation disorder preeclampsia. This is supported by recent studies of women with type 1 diabetes who develop preeclampsia, where decreased serum levels of DBP were also observed (Kelly, et al. 2020). In this report the lower circulating levels of DBP were assessed in the context of free and bound vitamin D metabolite levels, but direct actions of DBP may also occur in these women. Thus, circulating DBP may be a novel marker of preeclampsia risk. However, use of DBP as a systemic actin scavenger has also been proposed as strategy for the prevention of endothelial injury associated with bone marrow transplantation (Luebbering et al. 2020). It is therefore interesting to speculate that restoration of low serum DBP in pregnant women may provide a new approach for the management of disorder of placentation such as preeclampsia.

Declaration of interest, Funding and Acknowledgements

The authors would like thank Prof. Louise Kenny (University College Cork) for facilitating access to the SCOPE samples. They would also like to acknowledge help from Prof. Cedric Shackleton in establishing the urinary vitamin D metabolite analyses. The authors declare that there is no conflict of interest that could be perceived as prejudicing the impartiality of the research reported.

468 **Figure legends**

469 **Figure 1. Expression of VDR and DBP in trophoblasts and thyroid cells.** 1A. Expression of
470 protein for the vitamin D receptor (VDR, pink) and vitamin D binding protein (DBP, red) in JEG3,
471 BeWo, HTR8 and TPC cells cultured on Matrigel in the presence or absence of 1,25D (10 nM, 48
472 h). Immunofluorescence for each protein is shown in combination with nuclear (Hoechst, blue)
473 and membrane (NaK ATPase, green) markers. 1B. Data for total corrected cell fluorescence of
474 VDR and DBP protein expression (mean ± 95% CI) are shown for duplicate images from n= 3-4
475 separate experiments. Statistically different from vehicle-treated control, * $p < 0.05$, ** $p < 0.01$,
476 *** $p < 0.001$.

477

478 **Figure 2. Effects of 1,25D on trophoblasts and TPC cells cultured on Matrigel.** 2A.
479 Expression of mRNA (1/δCt) for *CYP24A1,* and 2B. Cell proliferation (BrdU incorporation,
480 absorbance units) (A) in JEG3, BeWo, HTR8 and TPC cells cultured on Matrigel in the presence
481 or absence of 1,25D (100 nM, 48 h). 2C. Cell matrix invasion (cell number/field of vision) by JEG3,
482 BeWo, HTR8 and TPC cells cultured on Matrigel in the presence or absence of 1,25D (10 nM and
483 100 nM, 48 h). 2D. Expression of mRNA for matrix metalloproteinase 2 (*MMP2*) and tissue-
484 inhibitor of matrix metalloproteinase 1 (*TIMP1*) in JEG3, BeWo, HTR8 and TPC cells cultured on
485 Matrigel in the presence or absence of 1,25D (100 nM, 48 hrs). Data for mRNA expression are
486 mean ± 95% CI 1/δCt value for duplicate or single analyses from n=3 separate experiments. Data
487 for cell invasion and cell proliferation assays are mean ± 95% CI, for triplicate or quadruplicate
488 analyses from 3-5 separate experiments. Statistically different from vehicle-treated control, * $p <$
489 0.05, ** $p < 0.01$, *** $p < 0.001$.

490

491 **Figure 3. Effect of VDR knockdown on 1,25D-induced cell matrix invasion.** Effect of siRNA
492 knockdown of *VDR* on (3A) *VDR* mRNA expression in JEG3 cells (3B) VDR (pink) and DBP (red)
493 protein expression. Immunofluorescence for each protein is shown in combination with nuclear

494 (Hoechst, blue) and membrane (NaK ATPase, green) markers. Effect of siRNA knockdown of
495 *VDR* on (3C) cell matrix invasion (cell number/field of vision) by JEG3 and TPC cells cultured on
496 Matrigel in the presence or absence of 1,25D (100 nM, 48 h). Data for cell fluorescence are mean
497 ± 95% CI, for quadruplicate analyses from 4 separate experiments. Data for matrix invasion
498 fluorescence are mean ± 95% CI, for duplicate analyses from 3 separate experiments. Statistically
499 different from vehicle-treated control, *** $p < 0.001$.

500500

501 **Figure 4. Effect of serum DBP and megalin function on intracellular DBP and trophoblast**
502 **function.** 4A. Effect of wild type (DBP+/+) and DBP knockout (DBP-/-) mouse serum on DBP
503 (red) and megalin (pink) protein expression in Matrigel cultured JEG3 cells. Immunofluorescence
504 for each protein is shown in combination with nuclear (Hoechst, blue) and membrane (NaK
505 ATPase, green) markers. 4B. Total corrected cell fluorescence for DBP and megalin protein
506 expression 4C. Matrigel invasion. 4D. Expression of mRNA for *MMP2*, *TIMP1*, *VDR, DBP* and
507 *megalin (LRP2)* in JEG3 cells cultured in medium with DBP+/+ or DBP-/- serum in the presence
508 or absence of 1,25D (100 nM, 48 h). 4E, 4F and 4G. DBP and megalin immunofluorescence, and
509 Matrigel invasion, in JEG3 cells cultured in FBS-supplemented medium in the absence or
510 presence of the megalin inhibitor RAP (1 μM)). Data for immunofluorescence are the mean ± 95%
511 CI for duplicate analyses from n=4 separate experiments. Data for matrix invasion are the mean
512 ± 95% CI for duplicate or single analyses from n=3 separate experiments. Data for mRNA
513 expression are the mean ± 95% CI for single analyses from n=3 separate experiments.
514 Statistically different from vehicle-treated control, * $p < 0.05$, ** $p < 0.01$, *** $p < 0.001$, **** $p <$
515 0.0001.

516

517 **Figure 5. ERK kinase activity and responses to 1,25D in trophoblastic and thyroid cells.**
518 **5**A. Western blot analysis of cytoplasmic and nuclear ERK and pERK in JEG3, BeWo and TPC
519 cells treated with or without 1,25D (100 nM, 48 h) or ERK kinase inhibitor U0126 (1μM, 48 h). 5B.

520 Effect of ERK kinase inhibitor U0126 on pERK in JEG3 cells cultured on Matrigel with or without
521 1,25D (100 nM, 48 h). 5C. Effect of ERK kinase inhibitor U0126 on DBP (red) and VDR (pink)
522 protein expression in Matrigel cultured JEG3 cells. Immunofluorescence for each protein is shown
523 in combination with nuclear (Hoechst, blue) and membrane (NaK ATPase, green) markers. 5D.
524 Matrigel invasion by JEG3, BeWo, HTR8 and TPC cells treated with 1,25D (100 nM, 48 hrs) in
525 the presence or absence of the ERK kinase inhibitor U0126 and in the presence or absence of
526 1,25D (100 nM, 48 h). Data showing the number of matrix invading cells/field of vision are the
527 mean ± 95% CI for triplicate analyses from 3 separate experiments. Statistically different from
528 vehicle-treated control, ** $p < 0.01$, *** $p < 0.001$.

529529

530 Figure 6. G-actin, F-actin and megalin concentration with respect to serum DBP level and
531 presence of serum 1,25D (100 nM, 48 h). 6A. Effects of wild type mice (DBP +/+) and knockout
532 mice (DBP -/-) serum on expression level of F-actin (green), G-actin (red) and DBP (yellow) in
533 JEG3 and HTR8 cells. Immunofluorescence for each protein is shown in combination with nuclear
534 (Hoechst, blue) marker. 6B. Data for total corrected cell fluorescence of F-actin and G-actin
535 protein expression (mean ± 95% CI) for images from 6A, with n=3 separate experiments and
536 showing multiple replicates for each experiment. 6C. Ratio of total corrected cell fluorescence of
537 G-actin and F-actin protein expression (mean ± 95% CI) for JEG3 and HTR8 data from 6B.
538 Statistically different from DBP+/+ control, ** $p < 0.01$, *** $p < 0.001$.

539539

540 Figure 7. DBP from pregnancy serum samples defines matrix invasion by JEG3 cells, and
541 is decreased in women who later develop preeclampsia . 7A-Correlation of serum DBP,
542 1,25D, and 25D with Matrigel invasion by JEG3 cells cultured in medium supplemented with
543 pregnancy serum samples. 7B. Correlation of DBP adjusted for 1,25D or 25D with invasion of
544 Matrigel by JEG3 cells for n=14 pregnancy serum samples. R and p value are shown for each

545 graph. 7C. Concentration of DBP in first trimester serum samples from women who went on to
546 have normal healthy or preeclampsia pregnancies (n = 20 samples in each group).
547547

548 **Figure 8. Schematic representation of the actions of DBP and 1,25D on trophoblast**
549 **invasion.** DBP and 1,25D cooperate to promote matrix invasion by trophoblasts. Inhibition of
550 this cooperative mechanism by ablation of serum DBP, inhibition of ERK kinase or inhibition of
551 DBP-megalin endocytosis (X) increases cellular G-/F-actin ratio and decreases matrix invasion.
552552

553 **Supplemental Figure 1. Effect of ERK kinase inhibition on expression of VDR and DBP in**
554 **Matrigel cultures of BeWo and HTR8 cells.** Immunofluorescence analysis of expression of
555 protein for DBP (red) and VDR (pink) in BeWo and HTR8 cells cultured the presence or absence
556 of 1,25D (100 nM, 48 hrs) without or with the pERK inhibitor U0126. Nuclear (Hoechst, blue) and
557 membrane (NaKATPase, green) are also shown. Scale bar shows 20μm. Images were taken with
558 40x magnification.
559559

560 **Supplemental Figure 2. Expression of the vitamin D system and proliferation response in**
561 **trophoblastic cells cultured on plastic.** S2A. Expression of mRNA (1/δCt) for *VDR, CYP24A1*,
562 and *DBP* and S2B. Cell proliferation (BrdU incorporation, absorbance units) in JEG3, BeWo, and
563 TPC cells cultured on platic in the presence or absence of 1,25D (100 nM, 48 h). S2C. Expression
564 of protein for the vitamin D receptor (VDR, pink) and vitamin D binding protein (DBP, red) in JEG3
565 and TPC cells cultured on plastic in the presence or absence of 1,25D (100 nM, 48 h).
566 Immunofluorescence for each protein is shown in combination with nuclear (Hoechst, blue) and
567 membrane (NaK ATPase, green) markers. Data (mean ± 95% CI) are shown for n= 3-4 separate
568 experiments. Statistically different from vehicle-treated control, ** $p < 0.01$.
569569
570570

References

Akour AA, Kennedy MJ & Gerk P 2013 Receptor-mediated endocytosis across human placenta: emphasis on megalin. *Mol Pharm* **10** 1269-1278.

Akour AA, Kennedy MJ & Gerk PM 2015 The Role of Megalin in the Transport of Gentamicin Across BeWo Cells, an In Vitro Model of the Human Placenta. *AAPS J* **17** 1193-1199.

Baca KM, Govil M, Zmuda JM, Simhan HN, Marazita ML & Bodnar LM 2018 Vitamin D metabolic loci and preeclampsia risk in multi-ethnic pregnant women. *Physiol Rep* **6** e13468.

Bao BY, Yeh SD & Lee YF 2006 1alpha,25-dihydroxyvitamin D3 inhibits prostate cancer cell invasion via modulation of selective proteases. *Carcinogenesis* **27** 32-42.

Benis KA & Schneider GB 1996 The effects of vitamin D binding protein-macrophage activating factor and colony-stimulating factor-1 on hematopoietic cells in normal and osteopetrotic rats. *Blood* **88** 2898-2905.

Birn H, Vorum H, Verroust PJ, Moestrup SK & Christensen EI 2000 Receptor-associated protein is important for normal processing of megalin in kidney proximal tubules. *J Am Soc Nephrol* **11** 191-202.

Bodnar LM, Catov JM, Simhan HN, Holick MF, Powers RW & Roberts JM 2007 Maternal vitamin D deficiency increases the risk of preeclampsia. *J Clin Endocrinol Metab* **92** 3517-3522.

Burke KA, Jauniaux E, Burton GJ & Cindrova-Davies T 2013 Expression and immunolocalisation of the endocytic receptors megalin and cubilin in the human yolk sac and placenta across gestation. *Placenta* **34** 1105-1109.

Calvo M & Ena JM 1989 Relations between vitamin D and fatty acid binding properties of vitamin D-binding protein. *Biochem Biophys Res Commun* **163** 14-17.

Chakraborty S & Ain R 2018 NOSTRIN: A novel modulator of trophoblast giant cell differentiation. *Stem Cell Res* **31** 135-146.

Chan SY, Susarla R, Canovas D, Vasilopoulou E, Ohizua O, McCabe CJ, Hewison M & Kilby MD 2015 Vitamin D promotes human extravillous trophoblast invasion in vitro. *Placenta* **36** 403-409.

Chun RF 2012 New perspectives on the vitamin D binding protein. *Cell Biochem Funct* **30** 445-456.

Delanghe JR, Speeckaert R & Speeckaert MM 2015 Behind the scenes of vitamin D binding protein: more than vitamin D binding. *Best Pract Res Clin Endocrinol Metab* **29** 773-786.

Gomme PT & Bertolini J 2004 Therapeutic potential of vitamin D-binding protein. *Trends Biotechnol* **22** 340-345.

Gressner OA, Lahme B & Gressner AM 2008 Gc-globulin (vitamin D binding protein) is synthesized and secreted by hepatocytes and internalized by hepatic stellate cells through Ca(2+)-dependent interaction with the megalin/gp330 receptor. *Clin Chim Acta* **390** 28-37.

Jorgensen CS, Christiansen M, Norgaard-Pedersen B, Ostergaard E, Schiodt FV, Laursen I & Houen G 2004 Gc globulin (vitamin D-binding protein) levels: an inhibition ELISA assay for determination of the total concentration of Gc globulin in plasma and serum. *Scand J Clin Lab Invest* **64** 157-166.

Kalwat MA & Thurmond DC 2013 Signaling mechanisms of glucose-induced F-actin remodeling in pancreatic islet beta cells. *Exp Mol Med* **45** e37.

Kelly CB, Wagner CL, Shary JR, Leyva MJ, Yu JY, Jenkins AJ, Nankervis AJ, Hanssen KF, Garg SK, Scardo JA, et al. 2020 Vitamin D Metabolites and Binding Protein Predict Preeclampsia in Women with Type Diabetes. *Nutrients* **12** 2048.

Kew RR 2019 The Vitamin D Binding Protein and Inflammatory Injury: A Mediator or Sentinel of Tissue Damage? *Front Endocrinol (Lausanne)* **10** 470.

Kim RH, Ryu BJ, Lee KM, Han JW & Lee SK 2018 Vitamin D facilitates trophoblast invasion through induction of epithelial-mesenchymal transition. *Am J Reprod Immunol* **79** e12796.

Kumar R, Cohen WR, Silva P & Epstein FH 1979 Elevated 1,25-dihydroxyvitamin D plasma levels in normal human pregnancy and lactation. *J Clin Invest* **63** 342-344.

617 Liang X, Jin Y, Wang H, Meng X, Tan Z, Huang T & Fan S 2019 Transgelin 2 is required for embryo618 implantation by promoting actin polymerization. *FASEB J* **33** 5667-5675.
619 Longtine MS, Cvitic S, Colvin BN, Chen B, Desoye G & Nelson DM 2017 Calcitriol regulates immune genes 620 CD14 and CD180 to modulate LPS responses in human trophoblasts. *Reproduction* **154** 735-744.
621 Luebbering N, Abdullah S, Lounder D, Lane A, Dole N, Rubinstein J, Hewison M, Gloude N, Jodele S, 622 Perentesis KMR, et al. 2020 Endothelial injury, F-actin and vitamin-D binding protein after hematopoietic623 stem cell transplant and association with clinical outcomes. *Haematologica* **10** 3324.
624 Lundgren S, Carling T, Hjalm G, Juhlin C, Rastad J, Pihlgren U, Rask L, Akerstrom G & Hellman P 1997 Tissue625 distribution of human gp330/megalin, a putative Ca(2+)-sensing protein. *J Histochem Cytochem* **45** 383- 626 392.
627 Ma R, Gu Y, Zhao S, Sun J, Groome LJ & Wang Y 2012 Expressions of vitamin D metabolic components 628 VDBP, CYP2R1, CYP27B1, CYP24A1, and VDR in placentas from normal and preeclamptic pregnancies. *Am*629 *J Physiol Endocrinol Metab* **303** E928-935.
630 Misu S, Takebayashi M & Miyamoto K 2017 Nuclear Actin in Development and Transcriptional631 Reprogramming. *Front Genet* **8** 27.
632 Naidoo Y, Moodley J, Ramsuran V & Naicker T 2019 Polymorphisms within vitamin D binding protein gene633 within a Preeclamptic South African population. *Hypertens Pregnancy* **38** 260-267.
634 Nykjaer A, Dragun D, Walther D, Vorum H, Jacobsen C, Herz J, Melsen F, Christensen EI & Willnow TE 1999635 An endocytic pathway essential for renal uptake and activation of the steroid 25-(OH) vitamin D3. *Cell* **96**636 507-515.
637 Otterbein LR, Cosio C, Graceffa P & Dominguez R 2002 Crystal structures of the vitamin D-binding protein638 and its complex with actin: structural basis of the actin-scavenger system. *Proc Natl Acad Sci U S A* **99**639 8003-8008.
640 Ryan BA & Kovacs CS 2020 Maternal and fetal vitamin D and their roles in mineral homeostasis and fetal 641 bone development. *J Endocrinol Invest*.
642 Safadi FF, Thornton P, Magiera H, Hollis BW, Gentile M, Haddad JG, Liebhaber SA & Cooke NE 1999643 Osteopathy and resistance to vitamin D toxicity in mice null for vitamin D binding protein. *J Clin Invest* **103**644 239-251.
645 Skruber K, Read TA & Vitriol EA 2018 Reconsidering an active role for G-actin in cytoskeletal regulation. *J*
646 *Cell Sci* **131**.
647 Tamblyn JA, Jenkinson C, Larner DP, Hewison M & Kilby MD 2018 Serum and urine vitamin D metabolite 648 analysis in early preeclampsia. *Endocr Connect* **7** 199-210.
649 Tamblyn JA, Susarla R, Jenkinson C, Jeffery LE, Ohizua O, Chun RF, Chan SY, Kilby MD & Hewison M 2017 650 Dysregulation of maternal and placental vitamin D metabolism in preeclampsia. *Placenta* **50** 70-77.
651 Viloria K, Nasteska D, Briant LJB, Heising S, Larner DP, Fine NHF, Ashford FB, da Silva Xavier G, Ramos MJ,652 Hasib A, et al. 2020 Vitamin-D-Binding Protein Contributes to the Maintenance of alpha Cell Function and653 Glucagon Secretion. *Cell Rep* **31** 107761.
654 Wang TJ, Zhang F, Richards JB, Kestenbaum B, van Meurs JB, Berry D, Kiel DP, Streeten EA, Ohlsson C,655 Koller DL, et al. 2010 Common genetic determinants of vitamin D insufficiency: a genome-wide association656 study. *Lancet* **376** 180-188.
657 Wei SQ, Qi HP, Luo ZC & Fraser WD 2013 Maternal vitamin D status and adverse pregnancy outcomes: a 658 systematic review and meta-analysis. *J Matern Fetal Neonatal Med* **26** 889-899.
659 Zehnder D, Bland R, Walker EA, Bradwell AR, Howie AJ, Hewison M & Stewart PM 1999 Expression of 25-660 hydroxyvitamin D3-1alpha-hydroxylase in the human kidney. *J Am Soc Nephrol* **10** 2465-2473.
661 Zehnder D, Bland R, Williams MC, McNinch RW, Howie AJ, Stewart PM & Hewison M 2001 Extrarenal662 expression of 25-hydroxyvitamin d(3)-1 alpha-hydroxylase. *J Clin Endocrinol Metab* **86** 888-894.

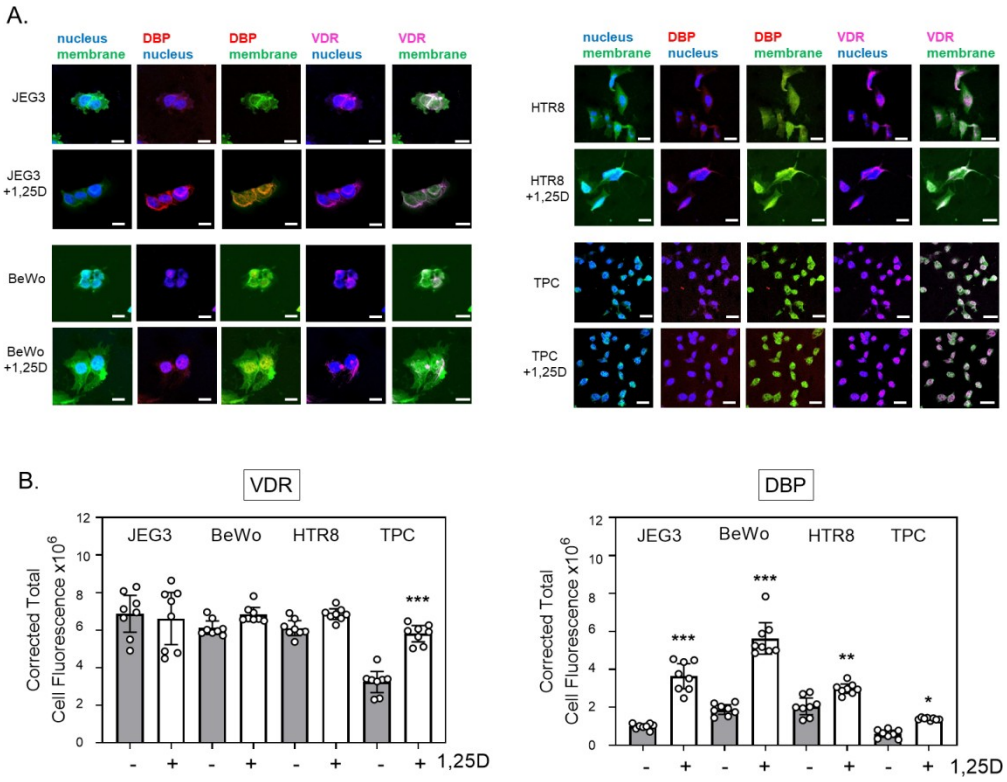

Figure 1

133x102mm (300 x 300 DPI)

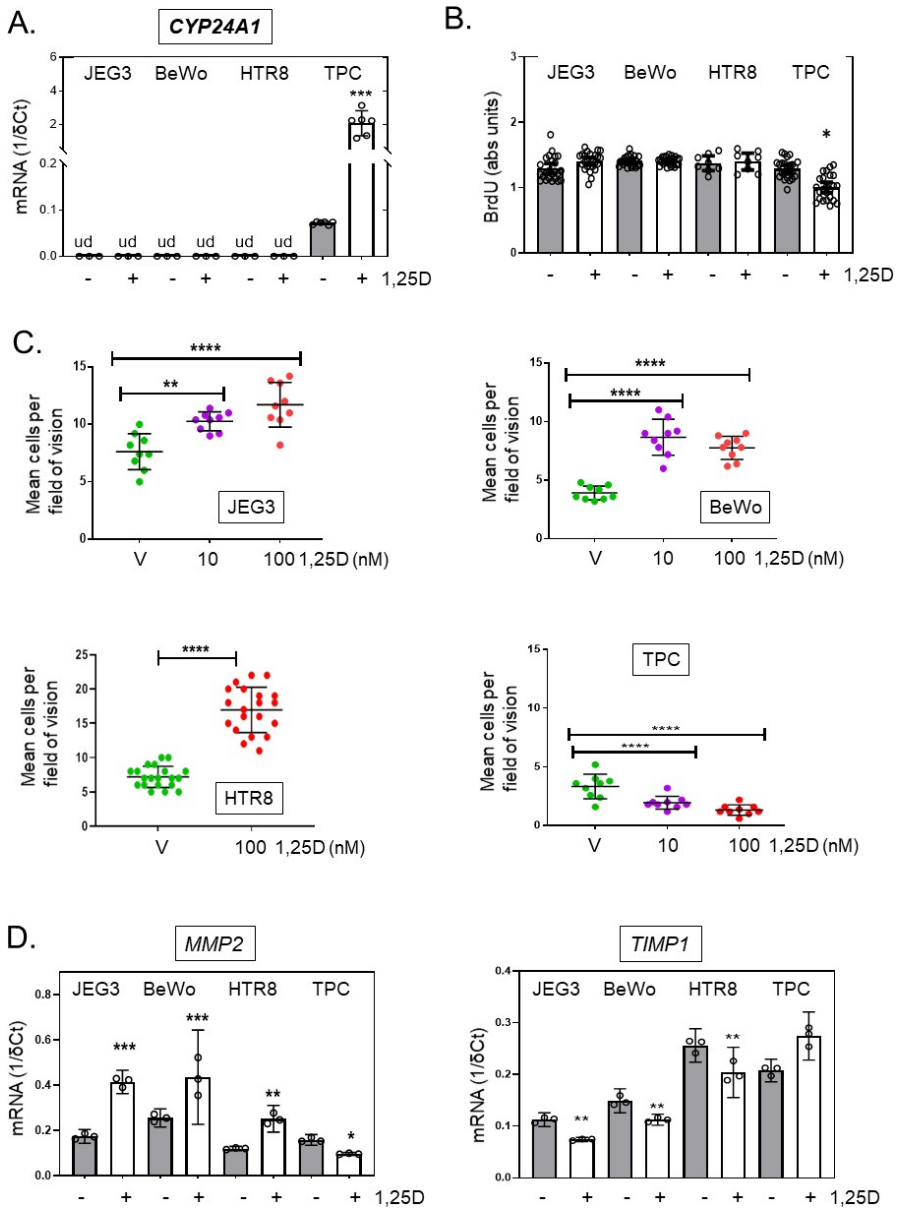

Figure 2

76x103mm (300 x 300 DPI)

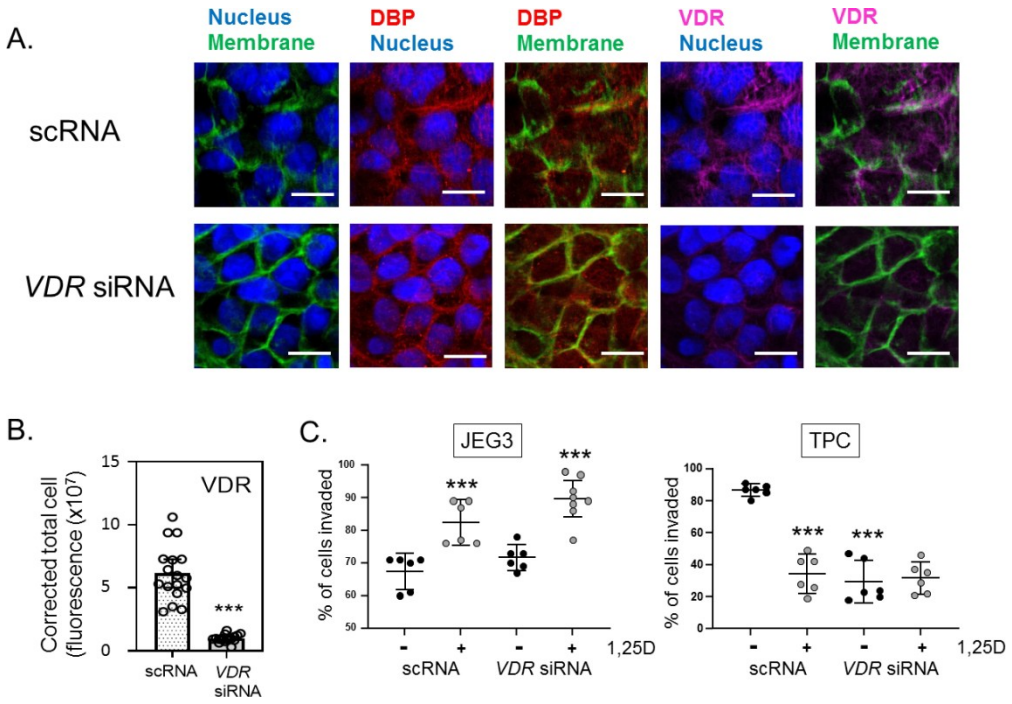

Figure 3

107x73mm (300 x 300 DPI)

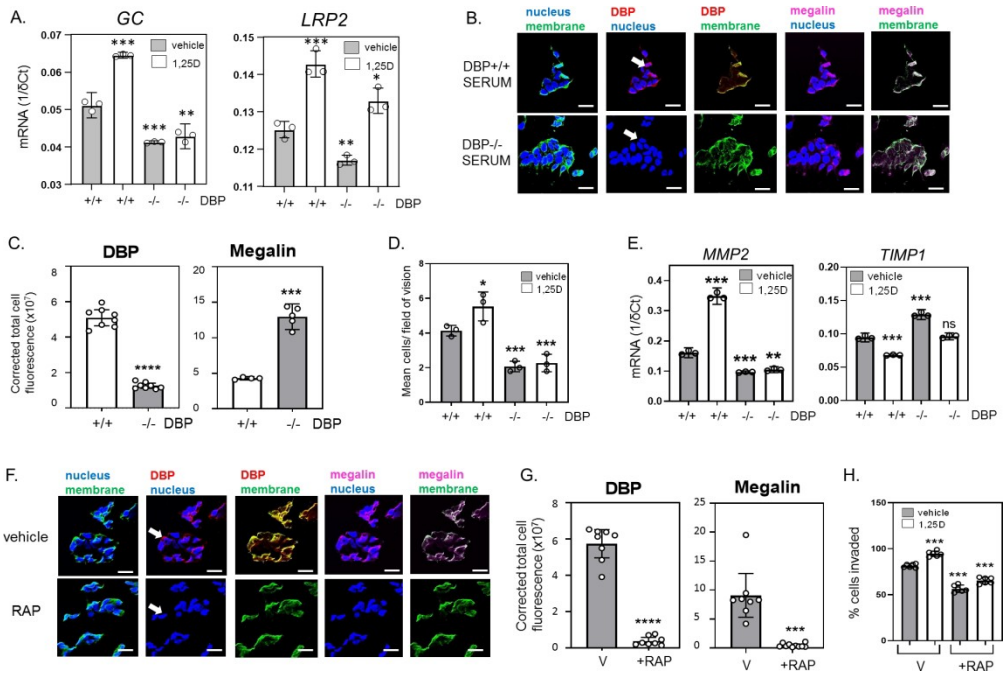

Figure 4

170x113mm (300 x 300 DPI)

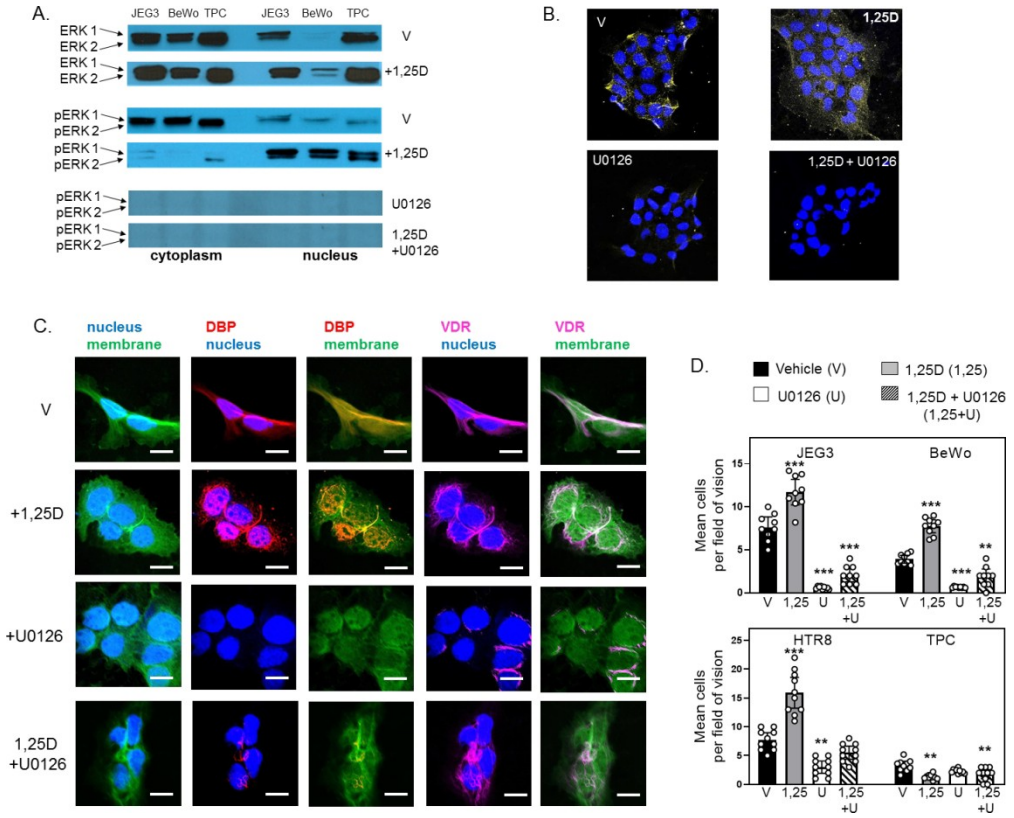

Figure 5

121x98mm (300 x 300 DPI)

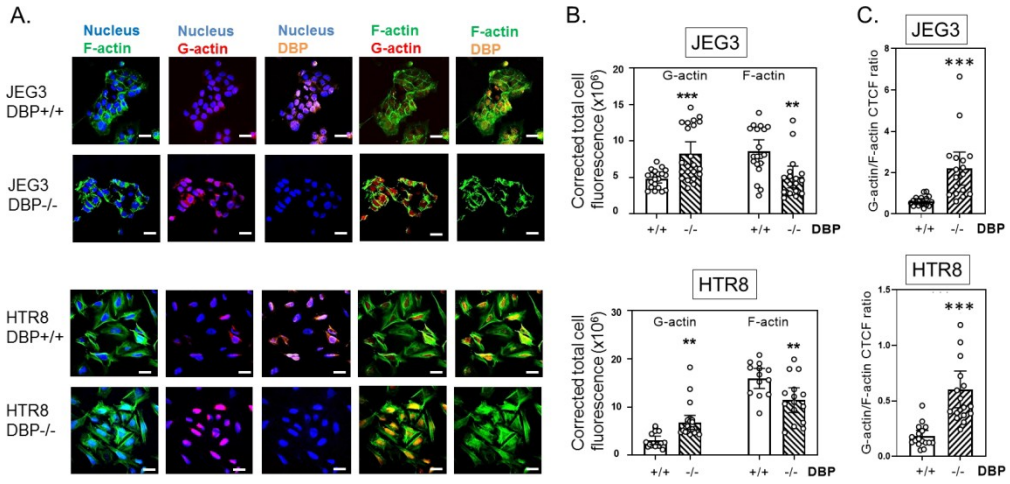

Figure

138x65mm (300 x 300 DPI)

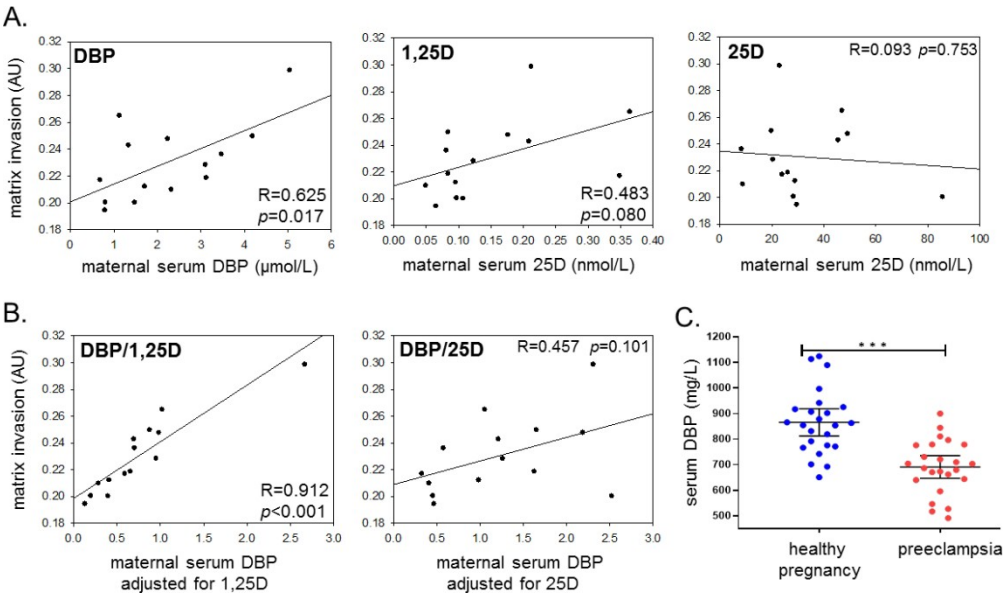

Figure 7

99x58mm (300 x 300 DPI)

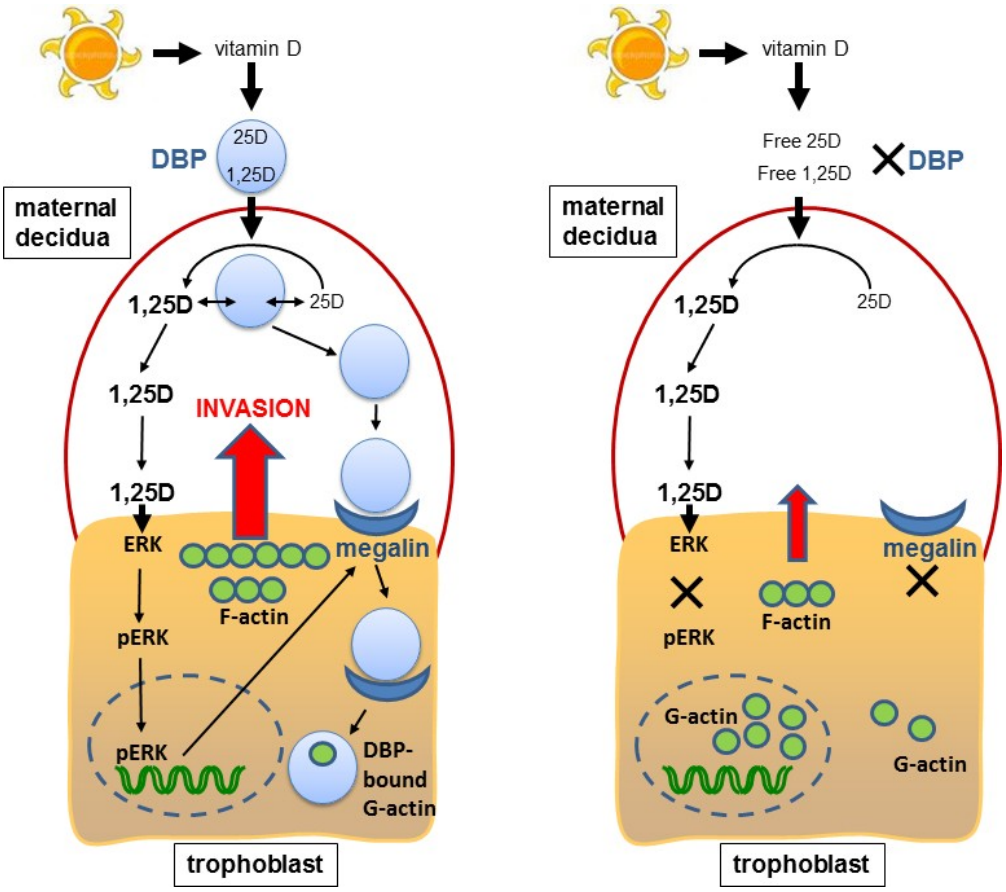

Figure 8

65x57mm (300 x 300 DPI)

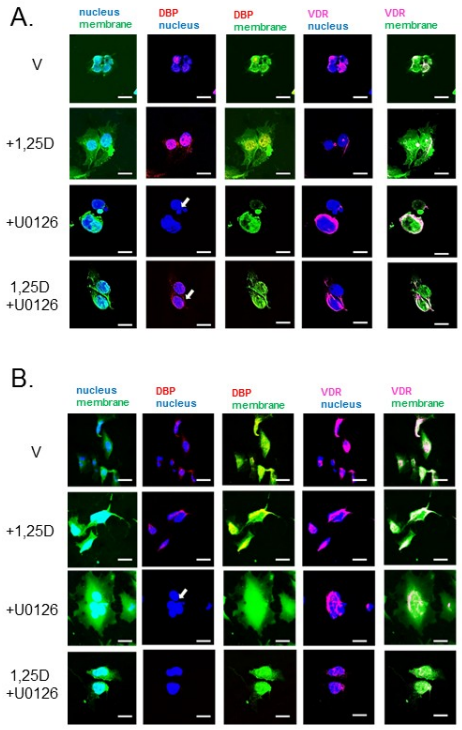

190x338mm (96 x 96 DPI)

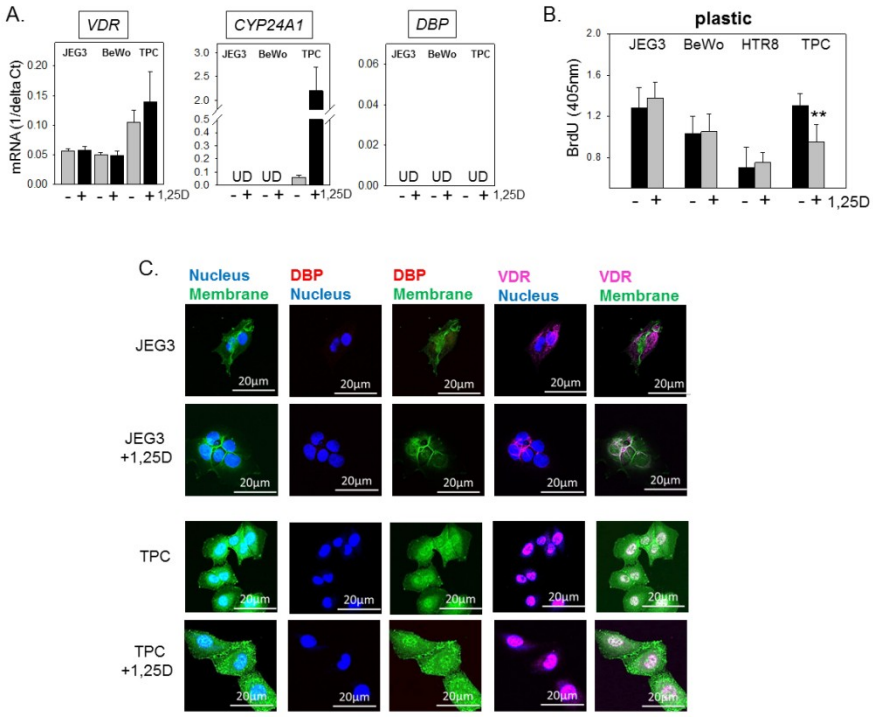

350x300mm (96 x 96 DPI)

Supplemental Table 1. Antibodies used in immunofluorescence analysis and Western blot analysis

Immunofluorescence analysis		
Primary antibodies	Manufacturer	Dilution used
anti-Vitamin D receptor (VDR)	Santa Cruz, D-6: sc-13133	1:50
anti-Vitamin D Binding protein	Abcam, ab65636	1:50
anti-LRP2 (Megalin)	Abcam, ab236244	1:50
anti-pERK1/2	Cell signalling, 9101L	1:50
anti-Sodium Potassium ATPase antibody-Plasma Membrane Marker Alexa Fluor 488 conjugate	Abcam, ab197713	1:100
Deoxyribonuclease-1. Alexa Fluor 594 Conjugate (anti-G-actin)	ThermoFisher, D12372	1:500
Phalloidin-. Alexa Fluor 488 conjugate (anti-F-actin)	Abcam, ab176753	1:500
Western blot analysis		
Primary antibodies	Manufacturer	Dilution used
anti-ERK1/2	ThermoFisher, MA5-15134, K.913.4	1:1000
anti-pERK1/2	ThermoFisher, MA5-15173, S.812.9	1:1000
anti-β-actin	Abcam, ab8227	1:10,000
Secondary antibodies		
Alexa Fluor 488 -conjugated goat anti-mouse IgG	ThermoFisher, A21235	1:250
Alexa Fluor 594 -conjugated goat anti-rabbit IgG	ThermoFisher, A11037	1:250